PROCEEDINGS OF SPIE

SPIEDigitalLibrary.org/conference-proceedings-of-spie

Passive indirect diffuse imaging

Yang, Shu, Lee, Kwan Kit, Ashok, Amit

Shu Yang, Kwan Kit Lee, Amit Ashok, "Passive indirect diffuse imaging," Proc. SPIE 11138, Wavelets and Sparsity XVIII, 111380U (9 September 2019); doi: 10.1117/12.2529956

SPIE.

Event: SPIE Optical Engineering + Applications, 2019, San Diego, California, United States

Passive indirect diffuse imaging

Shu Yang[a], Kwan Kit Lee[a], and Amit Ashok[a,b]

[a]1630 E University Blvd., James C. Wyant College of Optical Science
University of Arizona, Tucson, AZ, USA, 85721

[b]1230 E Speedway Blvd., Department of Electrical and Computer Engineering
University of Arizona, Tucson, AZ, USA, 85721

ABSTRACT

A passively illuminated scene presents a variety of photon pathways: direct and indirect, which convey varying levels of information about the scene across different dimensions of the light field. In indirect passive imaging, the object of interest is occluded from the imager which has no control over illumination. Using a second-order (non-linear) image formation model we demonstrate (experimentally) the feasibility of passive indirect diffuse imaging.

Keywords: Non-line-of-sight Imaging, Non-linear inverse problem, Passive imaging, Scattering

1. INTRODUCTION

Traditional passive imaging typically relies on direct (line-of-sight) photons emitted/reflected by an object for the image formation process. In a typical scene, light from an illumination source is reflected from object(s) of interest to the imager, which measures the direct (single-bounce) photons. In this work, we consider the problem of image formation where the scene/object of interest is occluded or outside the field-of-view (e.g. around the corner) of the imager. In such cases, the photons incident on the imaging aperture follow an an indirect (non-line-of-sight) path from the object, via intermediate reflecting/scattering surfaces, to the imaging aperture.[1,2] More specifically, here we consider scattering surfaces, such as white walls which are are optically rough, with a predominantly diffuse bi-directional reflectance function (BRDF). Our goal is to infer an unseen two-dimensional (2D) reflective pattern from the indirect photons gathered through one or more diffuse reflections. Using a second-order (non-linear) image formation model and maximum likelihood image reconstruction algorithm we demonstrate the feasibility of the indirect passive imaging with experimental results.

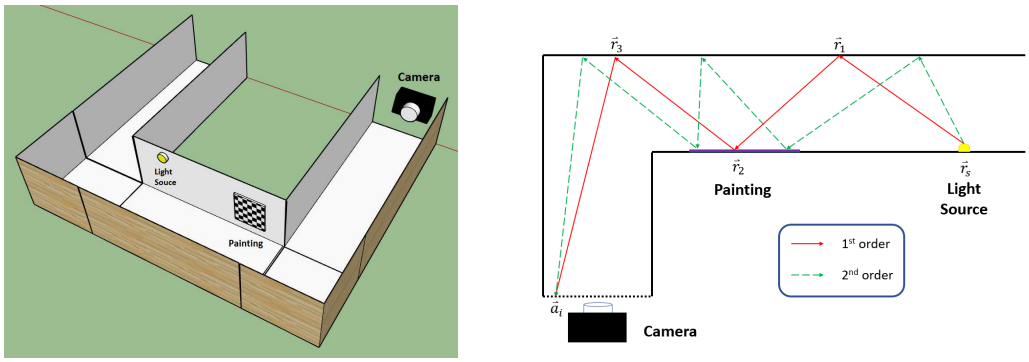

Figure 1. Schematic (left), and first-order/second-order photon pathways (right) of the representative hallway scene.

Further author information: Send correspondence to Amit Ashok E-mail: ashoka@optics.arizona.edu

Wavelets and Sparsity XVIII, edited by Dimitri Van De Ville, Manos Papadakis, Yue M. Lu, Proc. of SPIE
Vol. 11138, 111380U · © 2019 SPIE · CCC code: 0277-786X/19/$21 · doi: 10.1117/12.2529956

2. IMAGE FORMATION MODEL AND IMAGE RECONSTRUCTION

As shown in Fig. 1 (left), we consider a representative U-shape hallway scene, illuminated by a light small area white LED source, as an illustrative indirect imaging problem. In this case, the hallway walls are painted with scattering white pigment paint, which can be modeled by a micro-facet BRDF model.[3] For the image formation model, as shown in Fig. 1 (right), we consider the path of light rays, which begins at the light source and ends at the imaging aperture. Here we define the *order* of a light ray as the number of reflections, from the 2D reflective wall pattern, it undergoes before reaching the imaging aperture. For example, the first-order (Red) ray is reflected once and the second-order ray (Green dashed) is reflected twice off the 2D wall pattern, see Fig. 1 (right). We express the total detector plane measurement as a linear superposition of all the different orders of light rays yielding the following measurement $\vec{g}$ on the detector array:

$$g_i(\theta_1, \theta_2, ..., \theta_{n_p}) = m_i^{(0)} + \sum_{j=1}^{n_p} m_{i,j}^{(1)} \theta_j + \frac{1}{2} \sum_{j_1=1}^{n_p} \sum_{j_2=1}^{n_p} m_{i,j_1 j_2}^{(2)} \theta_{j_1} \theta_{j_2} + \frac{1}{3} \sum_{j_1=1}^{n_p} \sum_{j_2=1}^{n_p} \sum_{j_3=1}^{n_p} m_{i,j_1 j_2 j_3}^{(3)} \theta_{j_1} \theta_{j_2} \theta_{j_3} ...., \quad (1)$$

where g_i denotes the i^{th} detector pixel measurement, θ_j denotes the reflectivity of the j^{th} 2D wall pattern pixel, n_p is the total number of pixels on the 2D wall pattern, $m_i^{(k)}$ is the coefficient corresponding to the k^{th}-order light path. Thus, the coefficient $m_i^{(0)}$ represents all the photons measured at the i^{th} detector pixel that do not interact with the wall pattern. Similarly, the coefficient $m_{i,j}^{(1)}$ represents all the first order photon reflections from j^{th} 2D wall pattern pixel measured at the i^{th} detector pixel. For diffuse wall reflections, it is reasonable to approximate the aforementioned measurement model with up to second-order reflections to a good accuracy. This yields a second-order image measurement model:

$$g_i(\theta_1, \theta_2, ..., \theta_{n_p}) \approx m_i^{(0)} + \sum_{j=1}^{n_p} m_{i,j}^{(1)} \theta_j + \frac{1}{2} \sum_{j_1=1}^{n_p} \sum_{j_2=1}^{n_p} m_{i,j_1 j_2}^{(2)} \theta_{j_1} \theta_{j_2}. \quad (2)$$

Thus for any image detector pixel, we can use the parameters m, as defined in Eq. 2, to represent the physical forward-model. We we can express the m parameters collectively as a vector: $\vec{m} = [m_0, m_1, m_2, ..., m_{11}, m_{12}, ...]$. The image detector measurement vector can be defined as: $\vec{g}(\vec{\theta}) = [g_1(\vec{\theta}), g_2(\vec{\theta}), \cdots, g_N(\vec{\theta})]$, where $\vec{\theta} = [\theta_1, \theta_2, \cdots, \theta_{n_p}]$ represents the unknown pixelated 2D wall pattern reflectance. Our forward-model estimation utilizes the maximum likelihood (ML) principle.[4] We approximate the shot-noise limited measurement process with a Gaussian noise model yielding a maximum likelihood physical model estimation:

$$arg \min_{\vec{m}} \{ \left\| \vec{f_m} - \vec{f}(\vec{m}) \right\|^2 + \lambda \left\| \vec{m} \right\|^2 \} \quad s.t. \ \forall i \ m_i \geq 0 \quad (3)$$

Repeating the estimation process for every camera pixel provides the complete physical model of the imaging system: $M = (\vec{m}_1, \vec{m}_2, ...)$. For a given camera pixel we use a set of experimentally derived measurements of known 2D wall patterns to form an estimate of the forward-model parameters.

Our image reconstruction algorithm is based on the maximum likelihood principle to obtain an estimate of the 2D wall pattern subject to the binary constraint (dark/bright pixels):

$$arg \min_{\vec{\theta}} \ \left\| \vec{f}_{meas} - \vec{f}(M, \vec{\theta}) \right\|^2 \ \ s.t. \ \forall i \ \theta_i \in 0, 1 \quad (4)$$

We employ an experimentally derived forward-model (M) to compute the likelihood function. Subject to the binary constraint we compute the likelihood function for all possible 2D binary wall patterns and choose the one with the maximum likelihood.

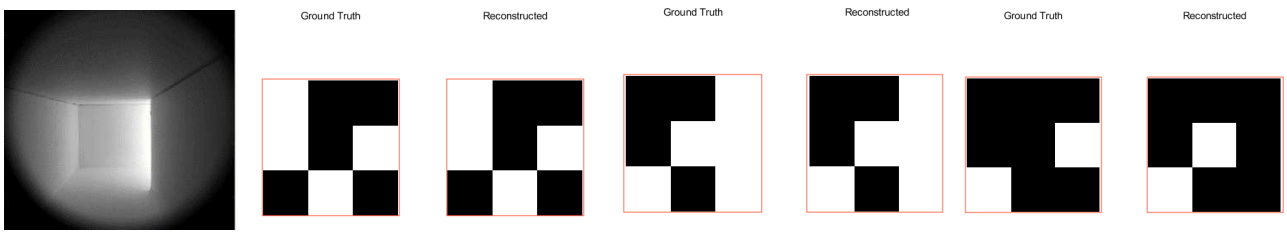

Figure 2. Example image measurement in hallway scene (left), and representative (binary) image reconstructions (right) results with varying levels of (pixel) errors obtained from experimental data for 3x3 2D wall patterns.

3. EXPERIMENTAL RESULTS

In our experimental study, we consider 3x3 or 4x4 pixellated 2D wall patterns for the image reconstruction problem. An E-Ink display is placed on one of the walls (shown as "painting" in Fig. 1), to serve a programmable 2D reflective pattern that can display a desired grayscale pixellated pattern. A high-dynamic range low noise sCMOS camera is used for image data acquisition.

For 3x3 reconstruction, we employ set of 250 grayscale 2D test patterns, displayed on the E-ink display, to estimate the second-order image formation model parameters. For the 3x3 wall patterns the number of relevant coefficients in our second-order image formation model for each detector pixel is 55, including one 0^{th} order coefficient, nine 1^{st} order coefficients, and forty-five 2^{nd} order coefficients. It is worth noting that while the second-order image formation coefficient estimates are about two orders of magnitude smaller than the first-order coefficients, the second-order coefficient are crucial to the success of image reconstruction process. Another disjoint set of 150 2D test patterns are used for the actual imaging performance analysis. Fig. 2 shows an example image measurement and three representative binary 2D wall patterns estimated from the experimental data. For binary 3x3 2D wall patterns, we record an average of 0.4 pixel errors out of 9 pixels for the tested binary patterns.

Note that for 4x4 reconstruction, there are 153 model parameters correspondingly, including one 0^{th} order coefficient, sixteen 1^{st} order coefficients and one hundred thirty-six 2^{nd} order coefficients. To deal with the difficulty introduced by the increased number of parameters, we increased the number of total measurement to 2000 and have used 1600 of them for model estimation, the rest of these measurements were used for testing. Fig. 3 shows a representative example of experimentally estimated forward-model parameters for 4x4 2D wall patterns. A five-fold cross validation is performed to verify effectiveness of this method. Fig. 3 shows some examples of reconstructed 4x4 patterns. We observe on average 1.5 pixel errors (out of 16 pixels) for the tested binary patterns. Note the the reconstruction fidelity (i.e. pixel error rate) does indeed increase with

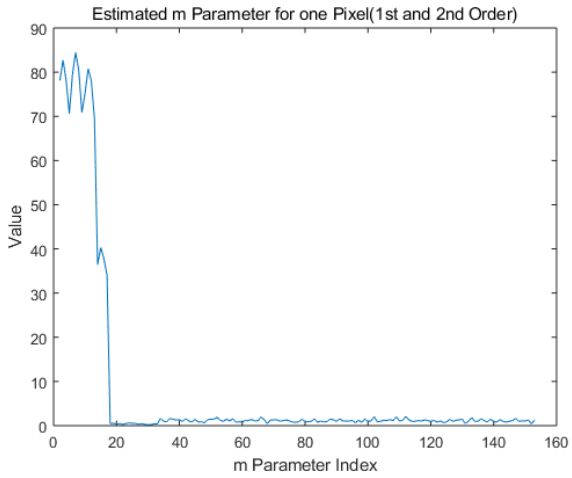

Figure 3. Example forward-model (experimentally derived) parameters for 4x4 2D wall patterns.

the complexity of the 2D wall patterns, e.g. in terms of increased spatial resolution from 3x3 to 4x4. This is expected as the distance in the measurement space (i.e. image measurement) between any two distinct wall patterns decreases (on average) with increasing spatial resolution while the measurement noise uncertainty remains relatively unchanged. Furthermore, some 2D wall patterns are more challenging to reconstruct versus other wall patterns due to the geometry of the hallway scene leading to non-uniform spatial resolution. Thus given the geometry of the hallway scene, the position of the illumination source (and its size and shape), the position of the painting, and the surface reflectivity (diffuse) of the walls there exists some inherent imaging resolution for given the source illumination strength and image measurement exposure time.

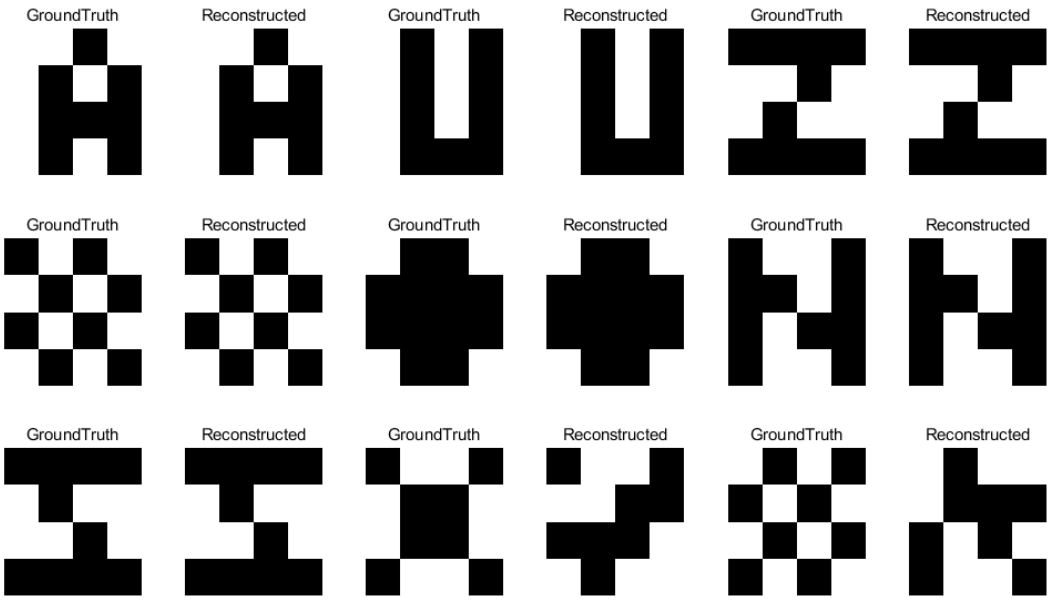

Figure 4. Example 4x4 original and reconstruction results obtained using experimental data.

4. CONCLUSIONS

In this work, we propose a second-order (non-linear) indirect passive image formation model for 2D image reconstruction from diffuse surface reflections. Using a ML reconstruction algorithm in conjunction wit our second-order (non-linear) image formation model, we experimentally demonstrate 2D image reconstructions of 3x3 and 4x4 binary 2D refelective patterns on a wall around a corner.

5. ACKNOWLEDGMENT

Authors gratefully acknowledge support from Defense Advanced Research Projects Agency (DARPA) REVEAL program under contract number HR0011-16-C-0026.

REFERENCES

[1] Y. Ding, A. Ashok, and S. Pau, "Real-time robust direct and indirect photon separation with polarization imaging," Optics Express **25**, 29432-29453 (2017).

[2] Y. Ding, R. Kerviche, A. Ashok, and S. Pau, "Eavesdropping of display devices by measurement of polarized reflected light," Applied Optics **57**, 5483-5491 (2018).

[3] S. D. Butler and M. A. Marciniak, "Robust categorization of microfacet BRDF models to enable flexible application-specific BRDF adaptation," Proc. SPIE 9205, 920506 (2014).

[4] J. W. Harris and H. Stocker, "Maximum Likelihood Method," Handbook of Mathematics and Computational Science, (Springer-Verlag 1998), pp. 824.